Liquefaction Evaluation for Rio Blanco Offstream Dam, Comparison Between Existing Methodologies

Evaluación del Potencial de Licuación para la Represa de Río Blanco, Comparación entre Metodologías Existentes

A. L. Fernandez and A. R. Crumley
GeoConsult, Inc. – Geotechnical Engineers, San Juan, Puerto Rico

Presented at Soil and Rock America,
12th Panamerican Conference on
Soil Mechanics and Geotechnical Engineering,
Cambridge, Massachusetts, June 2003

Abstract

This paper presents the liquefaction analysis conducted at the foundation of Rio Blanco Dam in Naguabo, Puerto Rico. The analyses follow a cyclic stress approach, and are based on CPT data. In addition, considering the location and the importance of Rio Blanco Dam, the assessment of the dynamic response of the soil deposits under strong motion excitation was an essential part of the design. The procedure for this investigation included:
(1) Definition of design earthquake; (2) Geotechnical characterization of the site, to define material properties of liquefiable layers; (3) Assessment of the residual or steady state strength of the liquefied soil. A critical state approach was included to assess the contractive behavior of the sand layers including mineralogical analyses to complement the measurement of critical state parameters.

Resumen

Este trabajo presenta los resultados de un estudio de licuación realizado para los suelos de fundación de la represa de Río Blanco, situada en Naguabo, Puerto Rico. Este análisis sigue un enfoque de esfuerzos cíclicos y esta basado en datos obtenidos de ensayos CPT. Asi mismo, dada a la importancia de la represa de Río Blanco, el estudio de respuesta dinámica de los depósitos de suelos bajo cargas sísmicas pasa a tomar una parte relevante del diseño. El procedimiento utilizado en esta investigación abarca: (1) Definición del sismo de diseño; (2) Caracterización geotécnica del área de la presa, a fin de definir las propiedades de los suelos licuables; (3) Estudio de la resistencia residual en estado crítico de los suelos licuables, la cual se incluyó para estudiar el comportamiento contractivo de los estratos arenosos, incluyendo un análisis mineralógico que complementa la definición de los parámetros de estado crítico.

1 SEISMICITY OF THE AREA

Puerto Rico is located within a seismically active zone at the northeastern boundary of the Caribbean Plate. The attenuation of earthquake waves is such that accelerations on the island from any of the active tectonic features should not exceed a value of 0.20g and is typically much lower. AASHTO has placed Puerto Rico in Zone 3, which imposes a maximum acceleration of 0.2g on bridge structures.

1.1 Definition of the Design Earthquake

The dynamic response analyses were conducted assuming a rockbase acceleration of 0.19g. After taking into account the uncertainty associated with the attenuation relation for rock accelerations in Puerto Rico, this value of pga = 0.19g in rock roughly relates to an earthquake with 10% probability of being exceeded in 50 years, which corresponds to a return period of 475 years. This is often referred as the 500-year earthquake or MPE (Maximum Probable Earthquake).

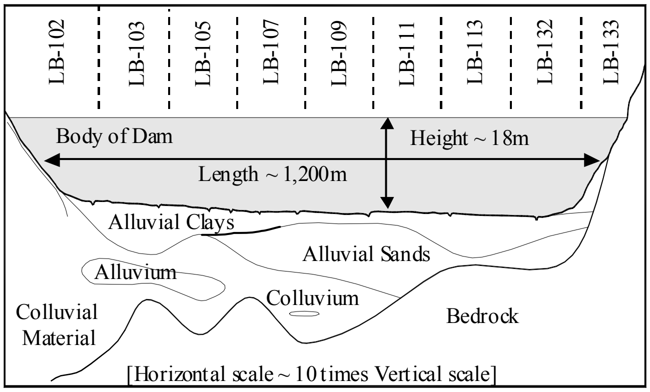

Figure 1 Geotechnical characterization for Rio Blanco Dam. Nine transverse profiles are defined

Table 1 Material properties (average values)

Material	Water content (%)	Plasticity Index (%)	Cohesion intercept (psf)	Friction angle (deg)
Alluvial clay	30-40	30-35	340-500	26-29
Colluvium (clay)	20-40	18-24	170-300	28-30
Alluvial sand	N/A	N/A	0-90	30-34

1.2 Dynamic Analysis

A site-specific design ground motion was performed on 9 soil profiles located along the proposed alignment of Rio Blanco Dam. Typical separation between soil profiles was about 120m. The geotechnical parameters were obtained from subsurface borings performed by GeoConsult. A summary of material properties is presented in Table 1 and a representation of the longitudinal profile is shown on Figure 1.

Peak ground acceleration and soil amplification at the surface level were computed using an equivalent linear procedure (program SHAKE91). The analyses included the mass of dam on top of the soil profile. Horizontal acceleration was computed at the base of the alluvial sand layers for the liquefaction analysis. The resulting response spectra were computed assuming a damping factor of 5%.

For a rockbase excitation of 0.19g, the resulting peak acceleration values at the base of the dam can be bounded within an upper limit of 0.40g.

Changes in the design level for the dam, led to a retrofit of the analyses in order to guarantee the serviceability of the dam after the occurrence of an earthquake with a higher return period. Following the owner's request, an earthquake with 2500-years of return period, was used as the MCE (Maximum Credible Earthquake). This earthquake is associated with a 2% probability of being exceeded in 50 years.

Four soil profiles were re-analyzed for this rockbase excitation of 0.40g. As a result, it was found that peak ground acceleration was similar to the values obtained in the previous analyses (Figure 2). After reviewing acceleration values at each layer it was observed that high acceleration values produce high shear, dissipating energy of the wave propagating upwards. For this reason, higher rock base accelerations did not produce peak ground accelerations greater than about 0.40g on soft soil sites. This last statement is in agreement with the results presented by Idriss, 1990, for soft soil sites; it also agrees with the 1997 NEHRP and 1997 UBC code site coefficients adopted for seismic design of buildings on soft soils. Therefore, the liquefaction analysis computed with a pga of 0.40g at the soil ground surface is roughly consistent with a decision of using either the MPE or the MCE as a measure of the level of rock acceleration.

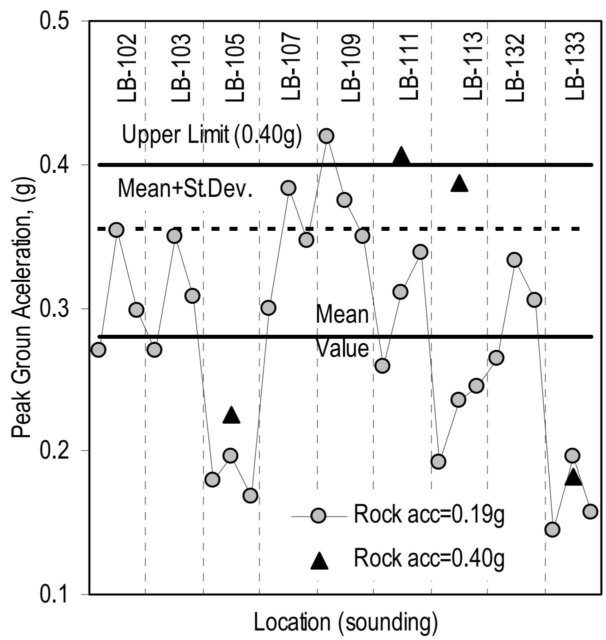

Figure 2 Dynamic response analysis of transverse soil profiles

2 LIQUEFACTION ANALYSIS

It is generally accepted that liquefaction potential of sandy layers can be evaluated using correlations between penetration resistance data, such as SPT and CPT, and the cyclic strength of the material mobilized during an strong motion shaking. In this study, CPT data was used because it provides the most reliable data on the relative density of sand deposits and provides a nearly continuous record of penetration resistance and sleeve friction. In this approach, the cyclic strength is characterized by the cyclic stress ratio (CSR). Basically, the CSR is the average shear stress (τ_{avg}) acting on a layer, normalized by the effective overburden stress (σ'_{vo}).

Prior SPT tests conducted on this site showed a large area with loose-to-medium sands under the footprint of the dam, near the left abutment (see Figure 3). It is in this area where additional CPT and downhole seismic tests were conducted to better define these potentially liquefiable layers.

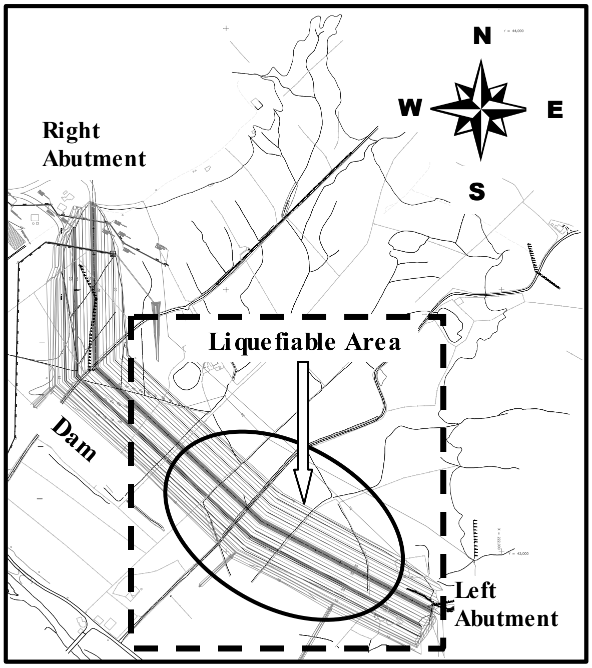

Figure 3 Identification of the liquefiable area

2.1 Cyclic Stress Approach

The liquefaction study performed for the Rio Blanco site follows a procedure presented by Schneider and Mayne (1999), which is based on the cyclic stress correlations initially developed by Seed and Idriss (1971 & 1987), and lately modified by Robertson and Wride (1997). According to these authors, CSR is a function of the earthquake duration (represented by the moment magnitude, M_w), the maximum horizontal acceleration (represented by the peak ground acceleration normalized by the acceleration of gravity, a_{max}/g), the depth of the granular deposit (represented by the stress reduction coefficient, r_d) and the normalized total vertical stress (ratio between total and effective stress acting on the layer, σ_{vo}/σ'_{vo}). Thus, CSR can be computed as:

$$CSR = \frac{\tau_{avg}}{\sigma'_{vo}} \approx 0.65 \cdot \left(\frac{a_{max}}{g}\right) \cdot \left(\frac{\sigma_{vo}}{\sigma'_{vo}}\right) \cdot r_d \tag{1}$$

r_d can be obtained using the following expression from Idriss (1999):

$$r_d = e^{[\alpha(z)+\beta(z)*M_w]} \tag{2}$$

Being z the depth in meters up to 25 m, and α and β are fitting functions defined as:

$$\alpha(z) = -1.01 - 1.06 \cdot \sin\left[\left(\frac{z}{11.73}\right) + 5.133\right] \tag{3}$$

$$\beta(z) = 0.106 + 0.118 \cdot \sin\left[\left(\frac{z}{11.28}\right) + 5.142\right] \tag{4}$$

The computed CSR values are compared with the cyclic resistance ratio, CRR, which defines a boundary where liquefaction is triggered.

CRR depends on the type penetration test used. For this study, the CRR is computed from CPT tests, based on the following Robertson and Wride (1998) correlations with the normalized tip resistance, q_{c1N} and assuming an earthquake of magnitude 7.5:

$$q_{c1N} = \frac{\left(q_c/Pa\right)}{\sqrt{\sigma'_{vo}/Pa}} = \frac{q_c}{\left(\sigma'_{vo} \cdot Pa\right)^{0.5}} \tag{5}$$

Pa: atmospheric pressure

For $(q_{c1N})_{cs} < 50$:

$$CRR_{7.5} = 0.83 \cdot \left(\frac{(q_{c1N})_{cs}}{1000}\right) + 0.05 \tag{6}$$

For $50 \leq (q_{c1N})_{cs} < 160$:

$$CRR_{7.5} = 93 \cdot \left(\frac{(q_{c1N})_{cs}}{1000}\right)^3 + 0.08 \tag{7}$$

Considering the large amount of CPT data gathered from the field exploration, the results of the liquefaction analysis were presented in two ways: (1) computing the factor of safety against liquefaction, and (2) computing the thickness of liquefiable layer (FS_L<1) at each soil.

The factor of safety against liquefaction, FS_L, was computed for every liquefiable layer in order to quantify its liquefaction potential. This factor of safety is defined as:

$$FS_L = \frac{CRR_{7.5}}{CSR} \tag{8}$$

As a result, FS_L lower than one (1) identifies liquefiable layers. It is important to comment that CSR depends directly on the magnitude of a_{max}. Therefore, to reduce uncertainties, this quantity must be determined based on “properly assessed” peak ground accelerations. For this study, the value of a_{max}=0.40g used for the analyses was obtained from 1-D dynamic analysis of a representative soil profiles.

Once FS_L was computed at every depth (considering only granular layers), the “liquefiable thickness”, H_L, was defined as the sum of all micro-layers within each soil profile with FS_L<1.

Then, computed H_L values were plotted at their corresponding CPT sounding location, and iso-curves were produced to interpolate the results between the soundings (see Figure 4). From these results, it is evident that liquefaction will occur over a major portion of the dam footprint for this ground acceleration value.

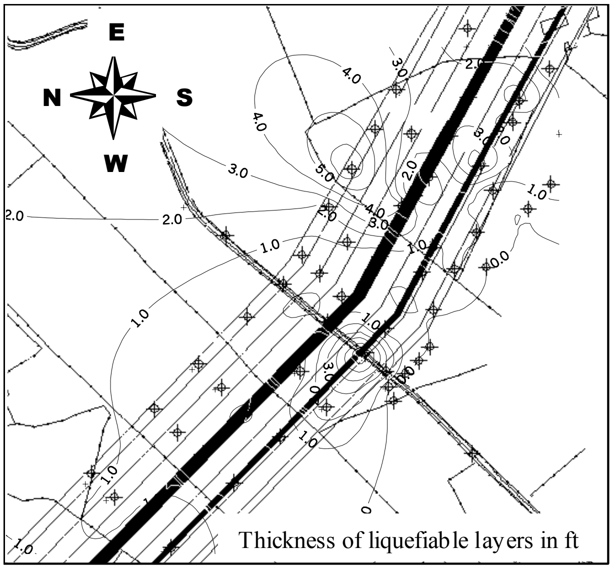

Figure 4 Thickness of liquefiable material for CPT-based liquefaction analysis

2.2 Vs-Based Liquefaction Assessment

The general accepted procedures to assess the liquefaction potential (correlations with SPT and CPT data) are based on cyclic induced-stresses. The basic assumption of this approach is that liquefaction resistance and in-situ penetration test resistance are functions of the relative density; therefore, they can be correlated.

On the other hand, Dobry et al. (1982) concluded that cyclic-induced strains are more significant than cyclic-induced stress to predict pore water pressure buildup and liquefaction. Thus, a low strain approach was followed for this part of the study. Shear wave velocity was measured in situ by seismic CPT downhole tests. These field mesurements are a very reliable source of data because they reflect the acting state of stress and are quickly performed. In addition, as G_{max} depends directly on Vs, there is a theoretical basis to correlate liquefaction resistance and Vs.

For this study, CRR was computed from a correlation with the overburden stress normalized shear wave velocity, Vs1, proposed by Andrus and Stokoe (1997):

$$CRR_{7.5} = 0.022 \cdot \left(\frac{V_{s1}}{100}\right)^2 + 2.8 \cdot \left(\frac{1}{V_{s1}^* - V_{s1}} - \frac{1}{V_{s1}^*}\right) \qquad (9)$$

with $V_{s1} = \dfrac{V_s}{(\sigma'_{vo})^{0.25}}$

$V_{s1}^* = 215$ m/s for fine content, FC $\leq$ 5%

$V_{s1}^* = [215 - 0.5(FC\text{-}5)]$ m/s for 5%<FC<35%

Although this approach seems to be more robust than the CPT-based approach, for this study it is being used only as a support tool. The reasons for this are that there are not enough data available to confidently cover the area in study, and there are not enough documented cases to verify the CRR curve. However, the location of the liquefiable areas (Figure 5) is in agreement with the CPT-based results. It is noted that the thickness of the liquefiable layers is significantly reduced using this approach, which might lead to potential savings in the remedial measures to control liquefaction.

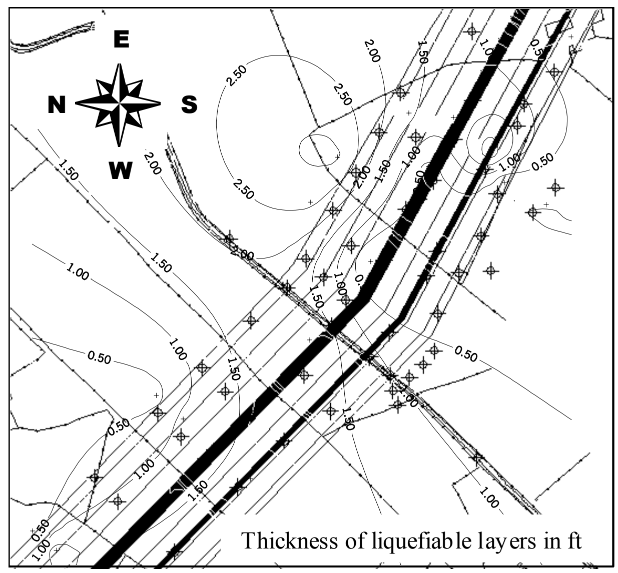

Figure 5 Thickness of liquefiable material for Vs-based liquefaction analysis

2.3 Critical State Approach

Initial triaxial test results from sand specimens taken near the left abutment showed high compressible behavior. Such outcome caused some concern about the dynamic behavior of this sand, specifically, whether or not this high compressibility of the sand would affect the liquefaction potential of the material.

Considering that the mineralogical structure plays a significant role in the contractive nature of sands, a set of X-RAY diffractometer tests was conducted in order to identify the mineralogical composition of those sand deposits at several locations in the area. Results showed a significant amount of K-feldspars (microclines, a prominent constituent of igneous rocks) on the compressible specimens. The presence of these minerals produces rounded particles that can be crushed under moderated stresses, increasing the compressibility of the material.

To support the results from the mineralogical characterization, GeoConsult-Georgia Tech and Golder & Associates tested several specimens from bulk samples (TPRB-26, TPRB-28, TPRB-32 and TPRB-33), which correspond to the specimens that showed some content of microclines. It was noted that most of the tested sands do not contain microclines, and therefore, did not show compressible behavior

A simplified procedure was used to determine the critical state line, CSL, for these specimens (Santamarina and Cho, 2001). The results are presented on Table 2. To validate these results, Golder ran a series of triaxial tests (drained and undrained), with very large deformations for one of the specimens (TPRB-26), which is in agreement with the results presented in this study.

According to critical state theory, the slope λ of the CSL has a direct correlation with the soil compressibility. In general, values of λ<0.07-009 are typical for silica and quartz sands. Higher values indicate more compressibility of the material, which may be due to particle shape/rearrangement or to grain crushing. In the case of Rio Blanco specimens, the critical state parameters presented in Table 2 show two well-defined compression behaviors for the sands. Specimens from TPRB-26, TPRB-28 and TPRB-32 show values of λ between 0.07 and 0.09, still suggesting a typical sand behavior. Conversely, specimens from TPRB-33 show large values of λ, between 0.15 and 0.16. In this case, high compressibility is expected from this material.

To further investigate the liquefaction risk of these sand specimens, Figure 6 shows a comparison between in situ condition and the corresponding critical state line for each specimen. Values of void ratio were derived from CPT data using Kulhawy and Mayne (1990)/Mayne and Kulhawy (1990) correlations from calibration chamber data:

$$e_o = 1.159 - 0.230 \cdot \log(q_{c1N}) \tag{10}$$

Results plotted in Figure 6 show a dilative behavior for specimens TPRB-28 and TPRB-32 implying the difficulty for the soil to flow in liquefaction. Conversely, the contractive behavior shown by specimen TPRB-33 suggests the susceptibility of this material to flow in liquefaction under the state of stress imposed by the dam. Finally, specimen TPRB-26 showed a partially contractive behavior, which insinuates certain liquefaction risk that has to be considered.

These results are in agreement with the peer review comments of this liquefaction study made by Dr. R. Dobry. He concluded that highly compressive sands might raise the pore water pressure under the dam, producing localized liquefaction.

Comparing the critical state assessment with the mineralogical analysis, it is observed that sand specimens containing K-feldspars show higher slope values of the CSL, indicating high compressibility of the material. The results are in good agreement with the triaxial test results. Conversely, quartz-silica sands showed low compressibility. It is noted that K-feldspars specimens were scarcely only found on the site.

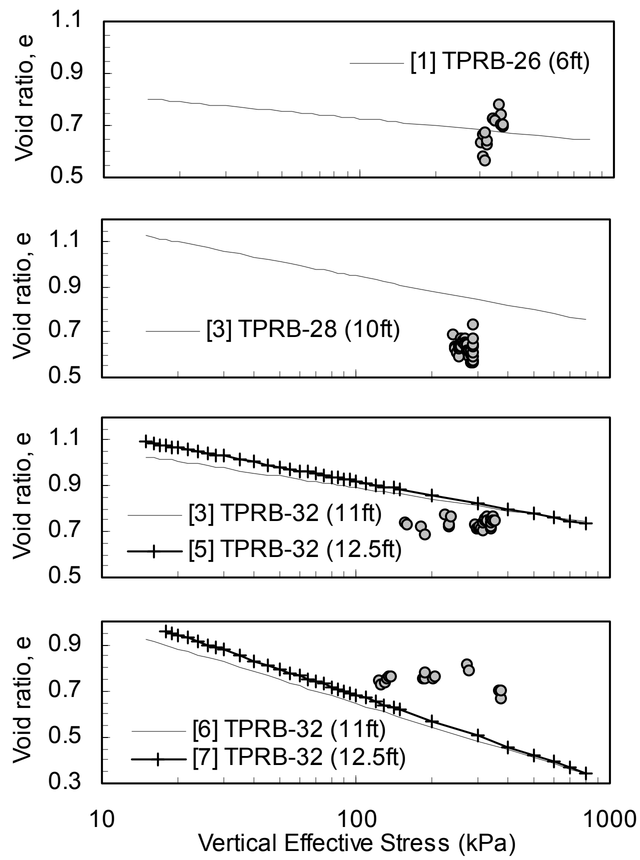

Figure 6 Critical state lines vs. in situ conditions at tests sites.

Table 2 Measured critical state parameters

Specimen	Depth ft	Intercept Γ	Slope λ
TPRB-28	10.0	1.38	0.09
TPRB-22	11.0	1.22	0.07
TPRB-32	12.0	1.33	0.09
TPRB-26	6.0	0.91	0.09
TPRB-33	7.5	1.32	0.15
TPRB-33	8.0	1.43	0.16

3 REMEDIAL MEASURES

Based on the results of the liquefaction analysis, it appears that the depth of liquefiable soils will generally be less than 20 feet. At present time, there are 3 options for which the economic feasibility is being evaluated: (1) dewatering, excavation, and replacement of liquefiable soils; (2) soil replacement using stone columns under the footprint of the dam; and (3) soil improvement by high energy compaction.

4 CONCLUSIONS

Considering the uncertainties on the spatial variability of the soil parameters and the soft nature of the upper layers along the dam, the assumed seismic scenario for the liquefaction analysis of the dam using a peak ground acceleration a_{max}=0.40 g appears to be unchanged for the MPE or the MCE. This pga value can be associated to the performance criterion where the structure needs to be serviceable within hours after the MPE.

According to the CPT-based evaluation the thickness of the liquefiable layer ranges from 4 to 7 feet.

The Vs-based and the CPT-based criteria for evaluating the liquefaction potential are generally consistent, and both show that locations near the left abutment have a higher liquefaction potential.

Critical state tests confirm the results of the mineralogical analysis, indicating that some sand specimens contain K-feldspar microclines, which produce a highly compressible behavior. The critical state evaluation of the liquefaction potential showed that some of the sand specimens present a dilative behavior, which affect their susceptibility to flow in liquefaction. To further evaluate the liquefaction effects of the specimens that showed contractive behavior, the evolution in time and space distribution should also be considered (e.g., the collapse of sand structures prevents liquefaction but can induce high pore water pressure over contiguous dilative materials).

From the CPT and Vs tests, it appears that the depth of liquefiable soils will generally be less than 20 feet. This result indicates that it may be feasible to dewater the dam footprint (or parts of the dam footprint) and then excavate the liquefiable soils, to replace with competent compacted material. The reconstructed trench could also form part of the impervious core, further reducing flows under the dam.

ACKNOWLEDGEMENT

Funding for this study was provided by the Puerto Rico Aqueduct and Sewer Authority, PRASA. The critical state tests were conducted in the Particulate Media Laboratory at Georgia Institute of Technology. The authors gratefully acknowledged their support, and also would like to show appreciation to Dr. Carlos Santamarina and Dr. Ricardo Dobry for their insightful comments.

REFERENCES

Andrus, R.D. and K. H. Stokoe (1999) “Liquefaction Resistance Based on Shear-Wave Velocity” Proceedings, Workshop on Evaluation of Liquefaction Resistance, MCEER-97-0022, Buffalo, NY. Pp.89-128

Building Seismic Safety Council (1998) “NEHRP Recommended Provisions for New Buildings” FEMA

Dobry, R., Ladd, R.S., Yokel, F.Y., Chung, R.M. and Powell, D. (1982) “Prediction of Pore Water Pressure Buildup and Liquefaction of Sands During Earthquakes by the Cyclic Strain Method” National Bureau of Standards Pub. NBS-138. July 1982

Finn, W.D.L. and Ledbetter, R.H. (1991) “Evaluation of Liquefaction Effects and remediation Strategies by Deformation Analysis” Proceedings of GEO-COAST ’91. Yokohama, Japan, pp. 441-446

Ishihara, K (1990) “Evaluation of Liquefaction Potential and Consequent Deformations in Sand Fills” Proceedings of the Workshop on Seismic Issues. Port of Los Angeles, CA.

Mayne, P.W. and Kulhawy, F.H. (1990). "Direct and Indirect Measurements of In-Situ Ko in Clays", Transportation Research Record 1278, Washington, D.C., pp. 141-149.

Kulhawy, F.H. and Mayne, P.W. (1990) # Manual on Estimating Soil Properties for Foundation Design, Report No. EL-6800, Electric Power Research Institute, Palo Alto, CA, August 1990, 306 p.

Robertson, P.K. and Wride, C.E. (1998) “Evaluating Cyclic Liquefaction Potential Using the Cone Penetration Test” Canadian Geotechnical Journal, 35 (3), pp.442-459

Santamarina, J.C. and Cho, G.C. (2001), Determination of Critical State Parameters in Sandy Soils - Simple Procedure, ASTM Geotechnical Testing Journal, vol. 24, no. 2, pp. 185-192

Santamarina, J.C., Fam, M. and Klein, K (2000) “Particulate Materials: Characterization with Elastic and Electromagnetic Waves” John Wiley & Sons.

Scheneider, J.A. and Mayne, P.W. (1999) “Soil Liquefaction Response in Mid-America Evaluated by Seismic Piezocone Tests” Mid-America Earthquake Center Report MAE-GT-3A. Georgia Institute of Technology, GA

Vucetic, M. and Dobry, R. (1991) “Effect of Soil Plasticity on Cyclic Response” ASCE Journal of Geotechnical Engineering. 117 (1). Pp. 89-1